Mitigation of Influenza B Epidemic with School Closures, Hong Kong, 2018

Sheikh Taslim Ali, Benjamin J. Cowling, Eric H.Y. Lau, Vicky J. Fang, Gabriel M. Leung

In winter 2018, schools in Hong Kong were closed 1 week before the scheduled Chinese New Year holiday to mitigate an influenza B virus epidemic. The intervention occurred after the epidemic peak and reduced overall incidence by ≈4.2%. School-based vaccination programs should be implemented to more effectively reduce influenza illnesses.

Hong Kong, China, located on the coast south of Guangdong Province, has a subtropical climate and a population of 7.3 million. In Hong Kong, influenza epidemics occur during winter every year and sometimes during other seasons (*1*). One of the interventions that has been used by Hong Kong health authorities to control influenza epidemics is school closures; this intervention was previously applied in 2008 (*2*) and 2009 (*3*). During winter 2017–18, an epidemic of influenza B, Yamagata lineage, occurred in Hong Kong. The local media focused on this epidemic for 3 reasons. First, the occurrence of severe influenza cases in Hong Kong (*4*) attracted public concern. Second, the number of school outbreaks reported to the Centre for Health Protection in Hong Kong far exceeded the number reported in previous years (*4*). Third, a severe epidemic of influenza A(H3N2) was ongoing in the United States (*5*), which further increased local concern about influenza in general.

On February 7, 2018, the Hong Kong government announced that all 1,600 kindergartens, primary schools, and special needs schools in Hong Kong would close the following day, 1 week before the Chinese New Year school holiday, which in most schools was scheduled for February 15–23. Thus, in total, schools were closed for 2.5 weeks. We reviewed surveillance data on influenza and influenza-like illness (ILI) activity in Hong Kong to infer the effect of school closures on community transmission.

The Study

As in previous studies, we used ILI surveillance data to indicate the incidence of influenza virus infections in the community (*1*,*6*,*7*). The Centre for Health Protection tracks a sentinel network of private doctors and reports the rates of outpatient consultations for ILI per 1,000 patient consultations every week (*4*), and the Public Health Laboratory Services branch reports the proportion of respiratory specimens testing positive for influenza virus by type and subtype every week (*8*). We multiplied the weekly ILI rates by the weekly influenza B virus detection rates to obtain a proxy (hereafter ILI+ proxy) measure of the number of cases of influenza B virus infection each week (Figure, panel A). We have previously shown that this ILI+ proxy provides an estimate that correlates linearly with the incidence of hospitalizations for influenza A(H1N1)pdm09 in Hong Kong (*6*); some have argued that this metric is a better linear correlate of the incidence of influenza illness than ILI rates alone or laboratory detection rates alone (*9*).

We calculated the ILI+ proxy for influenza B to infer the rate of person-to-person transmission of influenza B virus throughout the epidemic. We used the methods proposed by Cauchemez et al. (*10*) to estimate transmissibility by the effective reproduction number, R_t, which represents the average number of secondary infections that result from a primary case of infection at time *t* (online Technical Appendix, https://wwwnc.cdc.gov/EID/article/24/11/18-0612-Techapp1.pdf). When R_t exceeds 1, the epidemic is capable of spreading. We used flexible cubic splines to model the weekly influenza B ILI+ proxy values and interpolate daily ILI+ proxy values. We then estimated daily R_t values from the daily influenza B ILI+ proxy values (*7*). We considered the serial interval distribution as the Weibull distribution, with a mean of 3.2 days and SD of 1.3 days (*11*). The estimated R_t was 1.03 (95% CI 0.73–1.34) before the start of the school closure and 0.87 (95% CI 0.54–1.21) during the closure week, corresponding to a 16% (95% CI 10%–26%) reduction in transmissibility (Figure, panel B).

We then simulated the ILI+ proxy for influenza B under the counterfactual scenario of no school closures during February 8–14. Because R_t is affected by the depletion of the susceptible population (h_t, cumulative ILI+ proxy for influenza B at time *t*) and school closure (C_t, indicator variable at time *t*), we first fitted a multivariable log-linear regression model for R_t with h_t and C_t as explanatory variables (online Technical Appendix). Using these estimated coefficients in a regression model, we then constructed the transmission rate (β_t, function of initial transmission rate β_0 and C_t) for a susceptible-exposed-infected-recovered compartmental model to simulate incidence over time. To

Author affiliation: The University of Hong Kong, Hong Kong, China

DOI: https://doi.org/10.3201/eid2411.180612

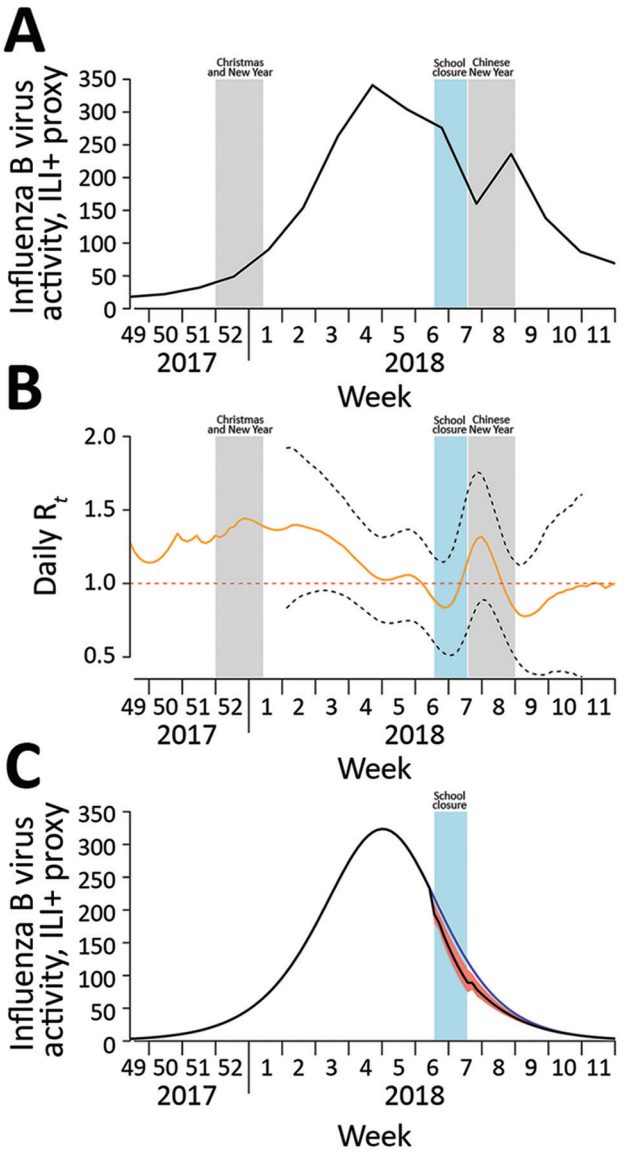

Figure. Influenza B virus activity, by epidemiologic week, Hong Kong, December 2017–March 2018. A) Incidence of influenza B virus measured by using the ILI+ proxy for influenza B, which is calculated by multiplying the weekly rate of ILI per 1,000 consultations by the weekly proportion of respiratory specimens submitted to the Public Health Laboratory Services (Hong Kong) that tested positive for influenza B virus (online Technical Appendix Table 2, https://wwwnc.cdc.gov/EID/article/24/11/18-0612-Techapp1.pdf). Shaded bars show school closure dates. B) Daily real-time estimate of transmissibility (R_t) of influenza B virus. Black dashed lines indicate pointwise 95% CIs; red dashed line indicates transmission threshold. Shaded bars show school closure dates. C) Simulated incidence of influenza B virus with and without implementation of school closure (shaded bar) in Hong Kong during February 8–14, 2018. Blue line indicates the number of cases occurring during the hypothetical scenario of no school closure; black line indicates the number occurring with school closure, which reduced transmissibility by 16%. The difference between these 2 lines represents the 4.2% reduction in incidence of infections; red shading indicates 95% CI. ILI, influenza-like illness; R_t, effective reproduction number at time *t*.

simulate incidence under no school closure, we set C_t to 0 for the period February 8–14 (online Technical Appendix).

Under the simulated epidemic with no school closures, the cumulative incidence for the entire epidemic was 0.527 (95% CI 0.472–0.574); the incidence was reduced to 0.505 (95% CI 0.494–0.519) when simulated with closures (Figure, panel C). This difference in proportions corresponds to a 4.2% (95% CI 1.5%–6.7%) reduction in infections from school closures. In sensitivity analyses, in which different levels of preexisting immunity (0.1%–30%) in the population were assumed, the estimated reduction in infections ranged from 3.3% (95% CI 1.2%–5.1%) for high (30%) preexisting immunity to 4.1% (95% CI 1.5%–6.7%) for low (0.1%) preexisting immunity. We also simulated the effect of school closures occurring 1 or 2 weeks earlier and estimated that infections would have been reduced by 8.6% if schools closed 1 week earlier (lasting for 2 weeks) and 13.5% if schools closed 2 weeks earlier (lasting for 3 weeks) (online Technical Appendix).

Conclusions

In early 2018, schools were closed an extra week before a holiday in Hong Kong to mitigate an influenza epidemic. Closure after the epidemic peak had a small effect on transmission; we estimated a 4.2% reduction in overall incidence of infections. By the end of the 2017–18 winter season, ≈400 laboratory-confirmed influenza deaths had occurred among the local population of 7.2 million, lower than the rate in the contemporaneous influenza A(H3N2) epidemic in the United States but still a rate of moderate-to-high impact. A reduction in incidence of infections by 4.2% might have reduced hospitalizations and deaths by a similar percentage, with the caveat that hospitalizations and deaths would probably not have been equally distributed among age groups because most infections occur in children and most deaths in older adults.

The school closures were announced <24 hours before they began. We presume that the school closures were disruptive to parents' schedules, potentially forcing some parents to stay home from work, and that many children stayed home during closures (*12*). The 16% reduction in transmission we estimated was lower than that estimated for the school closures that occurred in Hong Kong during June–July 2009 (25% reduction) (*3*). In 2009, the goal was to delay community transmission and spread out disease activity peak; thus, intervention before the peak was essential. In our study, R_t appeared to increase (Figure, panel B) during the Chinese New Year, probably because of increased social interactions during holiday gatherings.

We assumed that the ILI+ proxy for influenza B was linearly correlated with the incidence of infections (*1*,*6*,*7*). This correlation could have been affected by changes in healthcare seeking behavior that might have resulted from

private clinic closure, which occurred for a few days during the Chinese New Year holiday. This decreased healthcare access might have shifted the estimated reduction of influenza infections upward.

Influenza vaccination is considered the best preventive measure against influenza. However, >10 years after introduction of the influenza vaccination subsidy scheme for children, influenza vaccination coverage is still low in Hong Kong: ≈10% overall and ≈15% in children for the 2016–17 and 2017–18 winter seasons (*13*). To further increase influenza vaccination coverage in children, a school-based vaccination program should be implemented for the upcoming 2018–19 winter season.

Acknowledgments

The authors thank Julie Au and Huiying Chua for technical assistance.

This project was supported by the Harvard Center for Communicable Disease Dynamics from the National Institute of General Medical Sciences (grant no. U54 GM088558), a commissioned grant from the Health and Medical Research Fund from the Government of the Hong Kong Special Administrative Region, and the Research Grants Council of the Hong Kong Special Administrative Region, China (project no. T11-705/14N). The funding bodies had no role in study design, data collection and analysis, preparation of the manuscript, or the decision to publish.

About the Author

Dr. Ali works as a postdoctoral fellow at the World Health Organization Collaborating Centre for Infectious Disease Epidemiology and Control, School of Public Health, The University of Hong Kong in Hong Kong, China. His research interests include mathematical and statistical epidemiology, modeling of infectious diseases, and containment and mitigation policies.

References

1. Wu P, Presanis AM, Bond HS, Lau EHY, Fang VJ, Cowling BJ. A joint analysis of influenza-associated hospitalizations and mortality in Hong Kong, 1998–2013. Sci Rep. 2017;7:929. http://dx.doi.org/10.1038/s41598-017-01021-x
2. Cowling BJ, Lau EH, Lam CL, Cheng CK, Kovar J, Chan KH, et al. Effects of school closures, 2008 winter influenza season, Hong Kong. Emerg Infect Dis. 2008;14:1660–2. http://dx.doi.org/10.3201/eid1410.080646
3. Wu JT, Cowling BJ, Lau EH, Ip DKM, Ho LM, Tsang T, et al. School closure and mitigation of pandemic (H1N1) 2009, Hong Kong. Emerg Infect Dis. 2010;16:538–41. http://dx.doi.org/10.3201/eid1603.091216
4. Centre for Health Protection. Local situation of influenza activity (as of Feb 7, 2018). Flu Express. 2018;15:1–8.
5. Budd AP, Wentworth DE, Blanton L, Elal AIA, Alabi N, Barnes J, et al. Update: influenza activity—United States, October 1, 2017–February 3, 2018. MMWR Morb Mortal Wkly Rep. 2018;67:169–79. http://dx.doi.org/10.15585/mmwr.mm6706a1
6. Wong JY, Wu P, Nishiura H, Goldstein E, Lau EH, Yang L, et al. Infection fatality risk of the pandemic A(H1N1)2009 virus in Hong Kong. Am J Epidemiol. 2013;177:834–40. http://dx.doi.org/10.1093/aje/kws314
7. Ali ST, Wu P, Cauchemez S, He D, Fang VJ, Cowling BJ, et al. Ambient ozone and influenza transmissibility in Hong Kong. Eur Respir J. 2018;51:1800369. http://dx.doi.org/10.1183/13993003.00369-2018
8. Centre for Health Protection. Influenza virus subtyping in 2018. 2018 [cited 2018 Apr 4]. https://www.chp.gov.hk/en/statistics/data/10/641/643/6781.html
9. Goldstein E, Cobey S, Takahashi S, Miller JC, Lipsitch M. Predicting the epidemic sizes of influenza A/H1N1, A/H3N2, and B: a statistical method. PLoS Med. 2011;8:e1001051. http://dx.doi.org/10.1371/journal.pmed.1001051
10. Cauchemez S, Boëlle PY, Thomas G, Valleron AJ. Estimating in real time the efficacy of measures to control emerging communicable diseases. Am J Epidemiol. 2006;164:591–7. http://dx.doi.org/10.1093/aje/kwj274
11. Cowling BJ, Chan KH, Fang VJ, Lau LLH, So HC, Fung ROP, et al. Comparative epidemiology of pandemic and seasonal influenza A in households. N Engl J Med. 2010;362:2175–84. http://dx.doi.org/10.1056/NEJMoa0911530
12. Cauchemez S, Ferguson NM, Wachtel C, Tegnell A, Saour G, Duncan B, et al. Closure of schools during an influenza pandemic. Lancet Infect Dis. 2009;9:473–81. http://dx.doi.org/10.1016/S1473-3099(09)70176-8
13. Chiu SS, Kwan MYW, Feng S, Wong JSC, Leung CW, Chan ELY, et al. Interim estimate of influenza vaccine effectiveness in hospitalised children, Hong Kong, 2017/18. Euro Surveill. 2018;23. http://dx.doi.org/10.2807/1560-7917.ES.2018.23.8.18-00062

Address for correspondence: Benjamin J. Cowling, School of Public Health, Li Ka Shing Faculty of Medicine, The University of Hong Kong, 7 Sassoon Rd, Pokfulam, Hong Kong, China; email: bcowling@hku.hk

Article DOI: https://doi.org/10.3201/eid2411.180612

Mitigation of Influenza B Epidemic with School Closures, Hong Kong, 2018

Technical Appendix

log-Linear Regression Model for Real-Time Effective Reproduction Number R_t

The real-time effective reproduction number at time *t*, denoted by R_t, represents an instantaneous measure of transmissibility, defined as the average number of secondary infections generated by a typical primary infectious case at time *t*. When R_t exceeds 1, the epidemic will continue to spread. R_0 is the basic reproduction number (a measure of initial transmissibility), S_t is the proportion of susceptible individuals at time *t*, and I_t is the number of infectious cases at time *t*. Based on standard general epidemic theory, R_t depends on the initial intensity of disease transmission (i.e., R_0) and the proportion of susceptible individuals at that time *t* (i.e., S_t), i.e., $R_t = R_0 S_t$. Hence, R_t is the same as R_0 if all individuals are susceptible ($S_t = 1$), which sometimes happens at the beginning of an epidemic especially for a novel disease. Under the same condition, R_t will decrease over time when the susceptible population (S_t) becomes depleted. In reality, R_t might be modified by other factors, such as introduction of control measures. Here, we hypothesized that school closure (C_t) reduced transmissibility. Where C_t is an indicator variable defined as 1 for days under school closure and 0 for days not under school closure. This variable is modeled by a multiplier $e^{\lambda C_t}$, where λ is a coefficient indicating the effect of school closure. A negative λ indicates that school closure reduces R_t. Therefore, R_t can be expressed as $R_t = R_0 S_t e^{\lambda C_t}$ (equation 1). Also, $S_t = S_0 - h_t = S_0(1 + \alpha h_t)$; where, S_0 is the initial proportion of susceptible persons in the population, α (equal to $-1/S_0$) is a constant, h_t (equal to $\sum_{x=1}^{t-1} I_x$) is a variable indicating the depletion of susceptible persons in the population at time *t*. Using Taylor series expansion, we have $S_t \approx S_0 e^{\alpha h_t}$, then substitute into equation 1 and get the formula, $R_t = R_0 S_0 e^{\alpha h_t} e^{\lambda C_t}$. Taking logarithms of both sides, we reduce the formula, $\ln(R_t) = \ln(R_0 S_0) + \alpha h_t + \lambda C_t$, and finally simplified as $\ln(R_t) = K + \alpha h_t + \lambda C_t$ (equation 2), where $K = \ln(R_0 S_0)$ and α and

λ are regression coefficients for the depletion of susceptible persons and school closure, respectively.

Simulation of Influenza Activity by Susceptible-Exposed-Infected-Recovered (SEIR) Transmission Model

We simulated influenza activity by using the standard SEIR transmission model. The sets of differential equations that define the transmission model are $\frac{dS}{dt} = -\beta_t SI$, $\frac{dE}{dt} = \beta_t SI - \sigma E$, $\frac{dI}{dt} = \sigma E - \gamma I$, and $\frac{d\mathrm{R}}{dt} = \gamma I$, where *S*, *E*, *I*, and *R* denote the proportion of susceptible, exposed, infectious, and recovered persons, respectively. β_t is the transmission rate per infective case, which is a function of the effective reproduction number (R_t) as shown later. The rate of becoming infectious, σ, was set to value 0.625/d and the recovery rate, γ, to 0.763/d. With these values, the generation interval in the SEIR model is 3.2 days, a value that is typical for influenza virus (*1*). We chose the initial condition such that there was about a 2-week gap between the influenza B virus activity (influenza-like illness+ proxy for influenza B virus) peak and the start of the school closure. The simulation was carried out on the basis of the SEIR model, where the influenza activity is assumed to be proportional to *I*.

Based on the theoretical results of the SEIR model and relation between the transmission rate (β_t) and R_t, we have $\mathrm{R}_t = \frac{\beta_t}{\gamma} S_t$. Therefore, $\beta_t = \frac{\mathrm{R}_t}{S_t}\gamma = \mathrm{R}_0 \gamma e^{\hat{\lambda} C_t}$ (after substituting R_t from equation 1) = $\beta_0 e^{\hat{\lambda} C_t}$ (because $\beta_0 = \mathrm{R}_0\gamma$, when $S_0 \approx 1$). Hence, $\beta_t = \hat{\beta}_0\, e^{\hat{\lambda} C_t}$; therefore, $\hat{\beta}_0$ can be estimated once we estimate R_0.

Applying the multivariable log-linear regression model as described by equation 2, the regression coefficients ($\hat{K}$, $\hat{\alpha}$, and $\hat{\lambda}$) can be estimated. The value of S_0 represents the preimmunity in the population (e.g., $S_0 = 1$ indicates no preimmunity in the population). We reported results in the main text on the basis of no preimmunity. A sensitivity analysis was performed assuming different levels of preimmunity in the population (Technical Appendix Table 1). The estimated reduction in influenza B virus infections was shown to be robust over a plausible range of preimmunities. To simulate incidence under no school closure, we set $C_t = 0$ throughout the original school closure period.

Sensitivity Analysis

From the regression analysis, we found $\hat{\lambda}$ = –0.12 (95% CI –0.19 to –0.04) and $\widehat{K}$ = 0.345 (95% CI 0.302–0.388). By using formula $\widehat{K}$ = ln(R_0S_0), we find $R_0S_0 = e^{\widehat{K}}$ = 1.412. We assumed an immunity of 0.1%–30.1% at the start of the epidemic (i.e., reduced initial susceptibility) and performed the simulation under each scenario. We found a similar reduction in the infection rate during the implementation of a 1-week school closure in Hong Kong (Technical Appendix Table 1). Further, we also simulated the hypothetical impact of school closures 1 week or 2 weeks earlier, for 2 or 3 weeks total, respectively, and estimated that these school closures would have reduced the total infections by 8.6% or 13.5%, respectively.

Data Source

We used data on influenza virus from the Public Health Laboratory Services branch of the Centre for Health Protection, Hong Kong, and influenza-like illness activity using the sentinel influenza-like illness surveillance conducted by the Centre for Health Protection. We retrieved the data from https://www.chp.gov.hk/en/statistics/data/10/641/642/2274.html and https://www.chp.gov.hk/en/static/24015.html (Technical Appendix Table 2).

References

1. Cowling BJ, Chan KH, Fang VJ, Lau LLH, So HC, Fung ROP, et al. Comparative epidemiology of pandemic and seasonal influenza A in households. N Engl J Med. 2010;362:2175–84. PubMed http://dx.doi.org/10.1056/NEJMoa0911530

Technical Appendix Table 1. Sensitivity analysis of population with different preexisting influenza virus B immunities*

Preexisting immunity, %	S_0	R_0 (95% CI)	% Reduction of infections (95% CI)	School closure timing after peak, d
0.1	0.999	1.41 (1.35–1.48)	4.15 (1.48–6.70)	13
5.1	0.949	1.49 (1.43–1.55)	4.01 (1.43–6.47)	13
10.1	0.899	1.57 (1.50–1.64)	3.88 (1.38–6.22)	14
15.1	0.849	1.66 (1.59–1.74)	3.73 (1.33–5.97)	14
20.1	0.799	1.77 (1.69–1.84)	3.58 (1.28–5.70)	15
25.1	0.749	1.88 (1.81–1.97)	3.42 (1.22–5.43)	15
30.1	0.699	2.02 (1.93–2.11)	3.25 (1.16–5.14)	16

S_0, proportion susceptib**le; R_0**, **basic** reproductive number.

Technical Appendix Table 2. Incidence of influenza virus B–positive specimens and influenza-like illness, Hong Kong, October 2017–March 2018

Week	No. specimens tested	No. specimens influenza virus B–positive	GP ILI rate, per 1,000 consultations
2017 Oct 15–2017 Oct 21	3,653	41	43.7
2017 Oct 22–2017 Oct 28	3,348	50	40.1
2017 Oct 29–2017 Nov 4	4,171	62	37.8
2017 Nov 5–2017 Nov 11	3,891	54	43.8
2017 Nov 12–2017 Nov 18	3,780	48	39.5
2017 Nov 19–2017 Nov 25	3,667	58	43.2
2017 Nov 26–2017 Dec 2	3,792	69	35.4
2017 Dec 3–2017 Dec 9	3,882	85	41.4
2017 Dec 10–2017 Dec 16	4,094	104	42.4
2017 Dec 17–2017 Dec 23	4,085	172	38.5
2017 Dec 24–2017 Dec 30	4,518	343	32.2
2017 Dec 31–2018 Jan 6	4,692	528	39.8
2018 Jan 7–2018 Jan 13	5,105	681	57.8
2018 Jan 14–2018 Jan 20	7,176	1,346	70.0
2018 Jan 21–2018 Jan 27	7,562	1,681	76.8
2018 Jan 28–2018 Feb 3	7,399	1,492	75.4
2018 Feb 4–2018 Feb 10	8,350	1,614	71.3
2018 Feb 11–2018 Feb 17	6,322	1,391	36.4
2018 Feb 18–2018 Feb 24	9,638	1,978	57.4
2018 Feb 25–2018 Mar 3	7,363	1,064	47.9
2018 Mar 4–2018 Mar 10	6,375	692	40.2
2018 Mar 11–2018 Mar 17	5,655	430	45.3

GP, general practitioners, ILI, influenza-like illness.